
Diffusion Model Patching via Mixture-of-Prompts

Seokil Ham^{♣*} Sangmin Woo^{♣*} Jin-Young Kim[♡] Hyojun Go[♡]
 Byeongjun Park[♣] Changick Kim[♣]
[♣]KAIST [♡]Twelve Labs
[♣]{gkatjrldf, smwoo95, pbj3810, changick}@kaist.ac.kr
[♡]{gohyojun15, seago0828}@gmail.com
<https://sangminwoo.github.io/DMP/>

Abstract

We present Diffusion Model Patching (DMP), a simple method to boost the performance of pre-trained diffusion models that have *already reached convergence*, with a negligible increase in parameters. DMP inserts a small, learnable set of prompts into the model’s input space while keeping the original model frozen. The effectiveness of DMP is not merely due to the addition of parameters but stems from its dynamic gating mechanism, which selects and combines a subset of learnable prompts at every step of the generative process (*i.e.*, reverse denoising steps). This strategy, which we term “mixture-of-prompts”, enables the model to draw on the distinct expertise of each prompt, essentially “patching” the model’s functionality at every step with minimal yet specialized parameters. Uniquely, DMP enhances the model by further training on the same dataset on which it was originally trained, even in a scenario where significant improvements are typically not expected due to model convergence. Experiments show that DMP significantly enhances the converged FID of DiT-L/2 on FFHQ 256×256 by 10.38%, achieved with only a 1.43% parameter increase and 50K additional training iterations.

1 Introduction

The rapid progress in generative modeling has been largely driven by the development and advancement of diffusion models [17, 54], which have garnered considerable attention thanks to their desirable properties, such as stable training, smooth model scaling, and good mode coverage [40]. Diffusion models have set new standards in generating high-quality, diverse samples that closely match the distribution of various datasets [8, 45, 47, 51].

Diffusion models are characterized by their multi-step denoising process, which progressively refines random noise into structured outputs, such as images. Each step aims to denoise a noised input, gradually converting completely random noise into a meaningful image. Despite all denoising steps share the same goal of generating high-quality images, each step has distinct characteristics that contribute to shaping the final output [12, 42]. The visual concepts that diffusion models learn vary based on the noise ratio of input [6]. At higher noise levels (timestep t is close to T), where images are highly corrupted and thus contents are unrecognizable, the models focus on recovering global structures and colors. As the noise level decreases and images become less corrupted (timestep t is close to 0), the task of recovering images becomes more straightforward, and diffusion models learn to recover fine-grained details. Recent studies [2, 6, 12, 42] suggest that considering *stage-specificity* is beneficial, as it aligns better with the nuanced requirements of different stages in the generation process. However, many existing diffusion models do not explicitly consider this aspect.

Our goal is to enhance *already converged* pre-trained diffusion models by introducing stage-specific capabilities. We propose Diffusion Model Patching (DMP), a method that equips pre-trained diffusion

*Equal Contribution

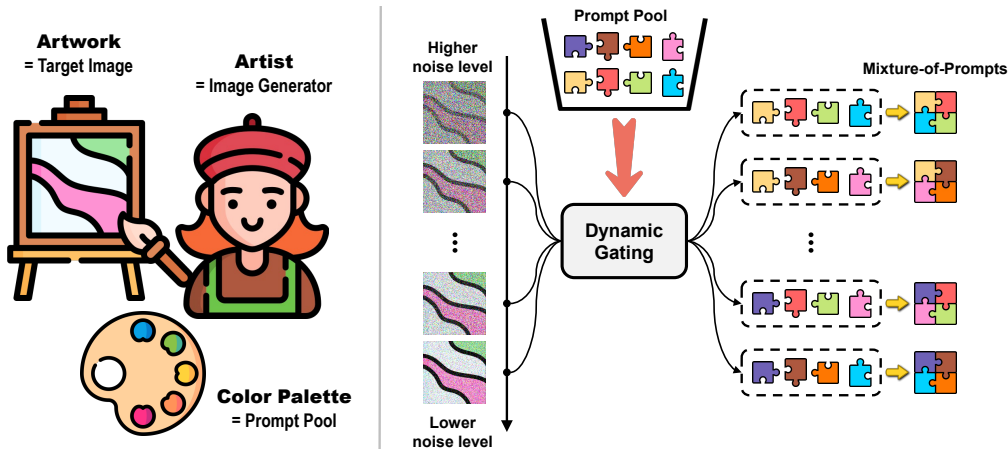


Figure 1: **Overview of DMP.** We take inspiration from prompt tuning [29] and aim to enhance *already converged* diffusion models. Our approach incorporates a pool of prompts within the input space, with each prompt learned to excel at certain stages of the denoising process. This is similar to giving a skilled artist an expanded color palette to refine different aspects of their artwork. At every step, a unique blend of prompts (*i.e.*, mixture-of-prompts) is constructed via dynamic gating based on the current noise level. This mechanism is akin to an artist choosing the appropriate color combinations for specific moments. Importantly, our method keeps the diffusion model itself unchanged, and we only use the original training dataset for further training.

models with an enhanced toolkit, enabling them to navigate the generation process with greater finesse and precision. An overview of DMP is shown in Fig. 1. DMP consists of two main components: (1) A small pool of learnable prompts [29], each optimized for particular stages of the generation process. These prompts are attached to the model’s input space and act as “experts” for certain denoising steps (or noise levels). This design enables the model to be directed towards specific behaviors for each stage without retraining the entire model, instead focusing on adjusting only small parameters at the input space. (2) A dynamic gating mechanism that adaptively combines “expert” prompts (or mixture-of-prompts) based on the noise levels of the input image. This dynamic utilization of prompts empowers the model with flexibility, enabling it to utilize distinct aspects of prompt knowledge sets at different stages of generation. By leveraging specialized knowledge embedded in each prompt, the model can adapt to stage-specific requirements throughout the multi-step generation process.

By incorporating these components, we continue training the converged diffusion models using the original dataset on which they were pre-trained. Given that the model has *already converged*, it is generally assumed that conventional fine-tuning would not lead to significant improvements or may even cause overfitting. However, DMP provides the model with a nuanced understanding of each denoising step, leading to enhanced performance, even when trained on the same data distribution. As shown in Fig. 2, DMP boosts the performance of DiT-L/2 [43] by 10.38% with only 50K iterations on the FFHQ [25] 256×256 dataset.

While simple, DMP offers several key strengths:

- ❶ **Data:** DMP boosts model performance using the original dataset, without requiring any external datasets. This is particularly noteworthy as further training of already converged diffusion models on the same dataset typically does not lead to performance gains. DMP differs from general fine-tuning [7, 41], which often transfers knowledge across different datasets.
- ❷ **Computation:** DMP patches pre-trained diffusion models by slightly modifying their input space, without updating the model itself. DMP contrasts with methods that train diffusion models from scratch for denoising-stage-specificity [6, 12, 14, 42], which can be computationally expensive and storage-intensive.
- ❸ **Parameter:** DMP adds only a negligible number of parameters, approximately 1.26% of the total model parameters (based on DiT-XL/2). This ensures that performance enhancements are achieved cost-effectively.

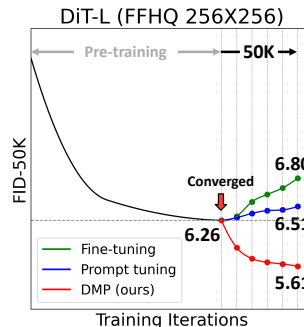


Figure 2: **Further training** of *fully converged* DiT-L/2. DMP achieves a 10.38% gain in FID-50K with only 50K iterations, while others overfit.

④ **Model:** DMP eliminates the need to train multiple expert networks for different denoising stages. Instead, it combines a few prompts in various ways to learn nuanced behaviors specific to each step. This simplifies the model architecture and training process compared to prior methods [2, 10, 66].

2 Related Work

Diffusion models with stage-specificity. Recent advancements in diffusion models [17, 54, 55] have broadened their utility across various data modalities, including images [47, 50], audios [27], texts [30] and 3D [62], showcasing remarkable versatility in numerous generation tasks. Recent efforts have focused on improving the specificity of denoising stages, with notable progress on both *architectural* and *optimization* fronts. (1) On the **architectural** front, eDiff-I [2] and ERNIE-ViLG 2.0 [10] introduced the concept of utilizing multiple expert denoisers, each tailored to specific noise levels, thereby augmenting the model’s overall capacity. Further, RAPHAEL [66] employed space-time experts, where space experts focus on specific image regions and time experts specialize in particular denoising stages. DTR [42] refined diffusion model architectures by allocating different channel combinations for each denoising step. (2) From an **optimization** perspective, Choi *et al.* [6] proposed a strategy to assign higher weights for stages constructing content and lower weights for stages cleaning up the remaining noise. Hang *et al.* [14] accelerated convergence by framing diffusion training as a multi-task learning problem [4], where loss weights are adjusted based on task difficulty at each timestep. Go *et al.* [12] mitigated learning conflicts of multiple denoising stages by clustering similar stages based on their signal-to-noise ratios (SNRs). Previous studies aim to improve the specificity of denoising stages, often by assuming either training from scratch or using multiple expert networks, which can be resource-intensive and require significant parameter storage. Our approach achieves stage-specificity *without* modifying the original model parameters, starting from and using only a single pre-trained diffusion model.

Parameter-efficient Fine-tuning (PEFT) in Diffusion models. PEFT offers a way to enhance models by tuning a small number of (extra) parameters, avoiding the need to retrain the entire model and significantly reducing computational and storage costs. This is particularly appealing given the complexity and parameter-dense nature of diffusion models [43, 48]. Directly training diffusion models from scratch is often impractical, leading to a growing interest in PEFT methods [63]. Recent advancements in this field can be broadly categorized into three streams: (1) T2i-Adapter [39], SCEdit [23], and ControlNet [69] utilize **adapters** [5, 19, 20] or **side-tuning** [57, 68] to modify the neural network’s behavior at specific layers, thereby rewriting activations. (2) Prompt2prompt [15] and Textual Inversion [11] use a concept similar to **prompt tuning** [22, 29, 31, 37, 71] that modifies input or textual representations to influence subsequent processing without changing the function itself. (3) CustomDiffusion [28], SVDiff [13], and DiffFit [64] focus on **partial parameter tuning** [32, 65, 67], fine-tuning specific parameters of the neural network, such as bias terms. These approaches have been successful in tuning diffusion models for personalization or customized editing, often using samples different from the original pre-training dataset [13, 15, 28, 49]. These have also been effective in enabling diverse conditional inputs for controllable image generation [23, 39, 69]. In contrast, our work aims to optimize the performance of pre-trained diffusion models with their original training datasets. While being parameter-efficient, our approach targets in-domain enhancements.²

3 Diffusion Model Patching (DMP)

We propose DMP³, a simple yet effective method aimed at enhancing *already converged* pre-trained diffusion models by enabling them to leverage knowledge specific to different denoising stages. DMP comprises two key components: (1) a pool of learnable prompts and (2) a dynamic gating mechanism. First, a small number of learnable parameters, referred to as prompts, are attached to the input space of the diffusion model. Second, the dynamic gating mechanism selects the optimal set of prompts (or mixture-of-prompts) based on the noise levels of the input image. Upon these components, we further train the model using the same pre-training dataset to learn prompts while keeping the backbone parameters frozen. We build upon the DiT [43] as our base model. The overall framework of DMP is shown in Fig. 3.

²Additional related work is in Appendix A.

³Preliminary of diffusion models is in Appendix B.

Prompt tuning. The core idea behind prompt tuning is to find a small set of parameters that, when combined with the input, effectively “tune” the output of a pre-trained model towards desired outcomes. Traditional fine-tuning aims to minimize the gap between ground truth \mathbf{y} and prediction $\hat{\mathbf{y}}$ by *modifying the pre-trained model* \mathbf{f}_θ , given the input \mathbf{x} :

$$\hat{\mathbf{y}}' = \mathbf{f}_{\theta'}(\mathbf{x}), \quad (1)$$

where $\hat{\mathbf{y}}'$ is the refined prediction, $\mathbf{f}_{\theta'}$ is the modified model, and the colors \bullet and \bullet indicate **learnable** and **frozen** parameters, respectively. This process is often computationally expensive and resource-intensive, as it requires storing and updating the full model parameters. In contrast, prompt tuning aims to enhance the output $\hat{\mathbf{y}}$ by directly *modifying the input* \mathbf{x} :

$$\hat{\mathbf{y}}' = \mathbf{f}_\theta(\mathbf{x}'). \quad (2)$$

Previous works [22, 29, 31, 61, 71] commonly define $\mathbf{x}' = [\mathbf{p}; \mathbf{x}]$, where $[\cdot; \cdot]$ denotes concatenation. However, we take a different approach by directly adding prompts to the input, aiming to more explicitly influence the input itself, thus $\mathbf{x}' = \mathbf{p} + \mathbf{x}$. Prompts are optimized via gradient descent, similar to conventional fine-tuning, but without changing the model’s parameters.

Motivation. During the multi-step denoising process, the difficulty and purpose of each stage vary depending on the noise level [6, 12, 14, 42]. Prompt tuning [22, 29, 31] assumes that if a pre-trained model already has sufficient knowledge, carefully constructed prompts can extract knowledge for a specific downstream task from the frozen model. Likewise, we hypothesize that a pre-trained diffusion model already holds general knowledge about all denoising stages, and by learning different mixture-of-prompts for each stage, we can patch the model with stage-specific knowledge.

3.1 Architecture

As our base architecture, we employ DiT [43], which is a transformer-based [59] DDPM [17] operating in the latent space [48]. We use a pre-trained VAE [26] from Stable Diffusion [48] to process input images into a latent code of shape $H \times W \times D$ (for $256 \times 256 \times 3$ images, the latent code is $32 \times 32 \times 4$). We then apply noise to latent code. The noisy latent code is divided into N fixed-size patches, each of shape $K \times K \times D$.

These patches are linearly embedded, and standard positional encoding [59] is applied to them, resulting in $\mathbf{x}^{(0)} \in \mathbb{R}^{N \times D}$. The patches are then processed by a sequence of L DiT blocks. These blocks are trained with a timestep embedding \mathbf{t} and optionally with class or text embedding. After the last DiT block, the noisy latent patches undergo the final Layer Normalization and are linearly decoded into a $K \times K \times 2D$ tensor (D for noise prediction and another D for diagonal covariance prediction). Finally, the decoded tokens are rearranged to match the original shape $H \times W \times D$.

Learnable prompts. Our goal is to efficiently enhance the model with denoising-stage-specific knowledge, focusing on adjusting small parameters within the input space. To achieve this, we start with a pre-trained DiT model and insert N learnable continuous embeddings of dimension D , *i.e.*, *prompts*, into the input space of each DiT block. The set of learnable prompts is denoted as:

$$\mathbf{P} = \{\mathbf{p}^{(i)} \in \mathbb{R}^{N \times D} \mid i \in \{0, \dots, L-1\}\}. \quad (3)$$

Here, $\mathbf{p}^{(i)}$ denotes the prompts for the i -th DiT block and L is the total number of DiT blocks in the model. Unlike previous methods [22, 29, 31, 61], where prompts are typically prepended to the input sequence, we directly add them to the input. This offers the advantage of not increasing the sequence length, thereby maintaining nearly the same computation speed as before. Moreover, during

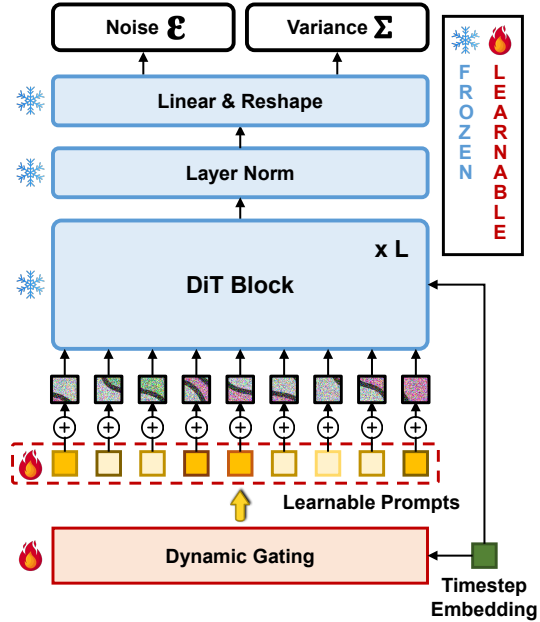


Figure 3: **DMP framework with DiT [43]**. DMP reuses the original dataset used to pre-train DiT.

the generation process, each prompt added to the input patch provides a direct signal to help denoise specific spatial parts at each timestep. This design choice allows the model to focus on different aspects of the input, aiding in specialized denoising steps. The output of i -th DiT block is computed as follows:

$$\mathbf{x}^{(i)} = \text{Block}^{(i)}(\mathbf{p}^{(i-1)} + \mathbf{x}^{(i-1)}). \quad (4)$$

During further training, only the prompts are updated, while the parameters of the DiT blocks remain unchanged.

Dynamic gating. In Eq. (4), the same prompts are used throughout the training, thus they will learn knowledge that is agnostic to denoising stages. To patch the model with stage-specific knowledge, we introduce dynamic gating. This mechanism blends prompts in varying proportions based on the noise level of an input image. Specifically, we use a timestep embedding \mathbf{t} to represent the noise level at each step of the generation process. For a given \mathbf{t} , the gating network \mathcal{G} creates mixtures-of-prompts, thereby redefining Eq. (4) as:

$$\mathbf{x}^{(i)} = \text{Block}^{(i)}(\sigma(\mathcal{G}(\mathbf{t}; i)) \odot \mathbf{p}^{(i-1)} + \mathbf{x}^{(i-1)}), \quad (5)$$

where σ is the softmax function and \odot denotes element-wise multiplication. In practice, \mathcal{G} is implemented as a simple linear layer. It additionally takes the DiT block depth i as input to produce different results based on the depth. This dynamic gating mechanism effectively handles varying noise levels using only a small number of prompts. It also provides the model with the flexibility to use different sets of prompt knowledge at different stages of the generation process.

3.2 Training

Zero-initialization. We empirically found that random initialization of prompts can disrupt the original information flow early in training, leading to instability and divergence. To ensure stable further training of a pre-trained diffusion model, we start by zero-initializing the prompts. With the prompt addition strategy that we selected before, zero-initialization helps prevent harmful noise from affecting the deep features of neural network layers and preserves the original knowledge at the beginning of training. In the first training step, since prompt parameters are initialized to zero, $\mathbf{p}^{(i-1)}$ term in Eq. (5) evaluates to zero, thus

$$\mathbf{x}^{(i)} = \text{Block}^{(i)}(\mathbf{x}^{(i-1)}). \quad (6)$$

As training progresses, the model can gradually incorporate additional signals from the prompts.

Prompt balancing loss. We adopt two soft constraints from Shazeer *et al.* [53] to balance the activation of mixtures-of-prompts. (1) Importance balancing: In a mixture-of-experts setup [21, 24], Eigen *et al.* [9] noted that once experts are selected, they tend to be consistently chosen. In our setup, the importance balancing loss prevents the gating network \mathcal{G} from overly favoring a few prompts with larger weights and encourages all prompts to have similar overall importance. (2) Load balancing: Despite having similar overall importance, prompts might still be activated with imbalanced weights. For instance, one prompt might be assigned with larger weights for a few denoising steps, while another might have smaller weights for many steps. The load balancing loss ensures that prompts are activated almost uniformly across all denoising steps (or noise levels).⁴

Prompt efficiency. Table 1 presents the model parameters for various versions of the DiT architecture [43] with and without the DMP, ranging from DiT-B/2 to DiT-XL/2 (where “2” denotes the patch size K). Assuming a fixed 256×256 resolution, using the DMP increases DiT-B/2 parameters by 1.96%. For the largest model, DiT-XL/2, the use of DMP results in a 1.26% increase to 683.5M parameters. The proportion of DMP parameters to total model parameters decreases as the model size increases, allowing for tuning only a small number of parameters compared to the entire model.

Model	#Parameters
DiT-B/2	130M
+ DMP	132.5M (+1.96%)
DiT-L/2	458M
+ DMP	464.5M (+1.43%)
DiT-XL/2	675M
+ DMP	683.5M (+1.26%)

Table 1: **Parameters.** Default image size is 256×256 .

⁴For further details about the prompt balancing loss, please refer to Appendix C.

FFHQ [7]		COCO [33]		ImageNet [25]	
Model	FID↓	Model	FID↓	Model	FID↓
<i>Pre-trained (iter: 600K)</i>		<i>Pre-trained (iter: 450K)</i>		<i>Pre-trained (iter: 7M)</i>	
DiT-B/2	6.27	DiT-B/2	7.33	DiT-XL/2	2.29
<i>Further Training (iter: 30K)</i>		<i>Further Training (iter: 40K)</i>		<i>Further Training (iter: 20K)</i>	
+ Fine-tuning	6.57(+0.30)	+ Fine-tuning	7.51(+0.18)	+ Fine-tuning	5.04(+2.75)
+ Prompt tuning	6.81(+0.54)	+ Prompt tuning	7.37(+0.04)	+ Prompt tuning	2.77(+0.48)
+ DMP	5.87(-0.40)	+ DMP	7.12(-0.21)	+ DMP	2.25(-0.04)

Table 2: **Patching the pre-trained DiT models [43] with DMP.** We set two baselines for comparison: (1) *conventional fine-tuning* to update the model parameters. (2) *naive prompt tuning* [29] (equivalent to Eq. (4)). Note that we use the same dataset as in the pre-training. ↑/↓: The higher/lower the better. Image Resolution is 256×256.

4 Experiments

We evaluate the effectiveness of DMP on various image generation tasks using pre-trained diffusion models that have *already converged*. Unlike conventional fine-tuning or prompt tuning, we use the same dataset for further training the model that was used in the pre-training phase. We evaluated image quality using FID [16] score, which measures the distance between feature representations of generated and real images using an Inception-v3 model [58].⁵

Datasets & Tasks. We used three datasets for our experiments: (1) FFHQ [25] (for *unconditional image generation*) contains 70,000 training images of human faces. (2) ImageNet [7] (for *class-conditional image generation*) involves 1,281,167 training images from 1,000 different classes. (3) MS-COCO [33] (for *text-to-image generation*) includes 82,783 training images and 40,504 validation images, each annotated with 5 descriptive captions.

4.1 Effectiveness of DMP

In Table 2, we present a comparison of DMP against two further training baselines – (1) traditional fine-tuning and (2) naive prompt tuning [29] (equivalent to Eq. (4)) – across three datasets for various image generation tasks. We employ pre-trained DiT models [43] that have already reached full convergence as our backbone. To ensure that the observed enhancement is not due to cross-dataset knowledge transfer, we further train the models using the same dataset used for pre-training. As expected, fine-tuning does not provide additional improvements to an already converged model in all datasets and can even result in overfitting. Naive prompt tuning also fails to improve performance in all datasets and can instead lead to a decrease in performance. DMP enhances the FID across all datasets with only 20~40K iterations, enabling the model to generate images of superior quality. This indicates that the performance gains achieved by DMP are not merely a result of increasing parameters, but rather from its novel mixture-of-prompts strategy. This strategy effectively patches diffusion models to operate slightly differently at each denoising step.

In Table 3, further training of a fully converged DiT-L/2 model reveals interesting dynamics. First, fine-tuning fails to increase performance beyond its already converged state and even tends to overfit, leading to performance degradation. We also found that prompt tuning, which uses a small number of extra parameters, actually harms performance, possibly because these extra parameters act as noise in the model’s input space. In contrast, DMP, which also uses the same set of parameters as prompt tuning, significantly boosts performance. The key difference between them lies in the use of a gating function: prompts are shared across all timesteps, while DMP activates prompts differently for each timestep. This distinction allows DMP, with a fixed number of parameters, to scale across thousands of timesteps by creating mixtures-of-prompts. By patching stage-specificity into the pre-trained diffusion model, DMP achieves a 10.38% FID gain in just 50K iterations.

Pre-trained DiT-L/2 (FID = 6.26)							
Further Training	0K	10K	20K	30K	40K	50K	
+ Fine-tuning	6.26	6.32	6.53	6.64	6.73	6.80	(+0.54)
+ Prompt-tuning	6.26	6.30	6.36	6.40	6.42	6.51	(+0.25)
+ DMP	6.26	5.88	5.72	5.67	5.64	5.61	(-0.65)

Table 3: **Comparison of further training techniques on FFHQ 256×256 [25].**

⁵Implementation details can be found in Appendix D.

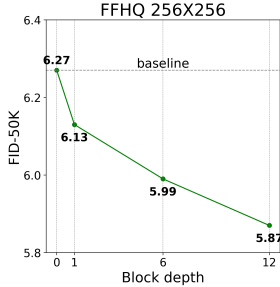


Figure 4: **Prompt depth.**

case	FID↓
attention	6.41
linear	5.87

(a) **Gating architecture.**

case	FID↓
uniform	5.97
distinct	5.87

(c) **Prompt selection.**

case	FID↓
hard	5.96
soft	5.87

(b) **Gating type.**

case	FID↓
prepend	6.79
add	5.87

(d) **Prompt position.**

IB	LB	FID↓
✗	✗	6.11
✓	✗	5.97
✗	✓	5.96
✓	✓	5.87

(e) **Prompt balancing.** IB: importance balancing; LB: load balancing.

Table 4: **DMP ablations.** DiT-B/2 [43] pre-trained on FFHQ 256×256 [25] is further trained for 30K iterations with DMP (Baseline FID = 6.27).

4.2 Design Choices

Prompt depth. To investigate the impact of the number of blocks in which prompts are inserted, we conduct an ablation study using the DiT-B/2 model, which comprises 12 DiT blocks. We evaluate the performance differences when applying mixtures-of-prompts at various depths in Fig. 4: only at the first block, up to half of the blocks, and across all blocks. Regardless of the depth, performance consistently improves compared to the baseline (FID=6.27) with no prompts. Our findings indicate a positive correlation between prompt depth and performance, with better results achieved using mixture-of-prompts across more blocks. The prompts selected for each block are illustrated in Fig. 5.

Gating architecture. Our DMP framework incorporates a dynamic gating mechanism to select mixture-of-prompts specialized to each denoising step (or noise level). We compare the impact of two gating architectures in Table 3a: linear gating *vs.* attention gating. The linear gating utilizes a single linear layer, taking a timestep embedding as input to produce a soft weighting mask for each learnable prompt. On the other hand, attention gating utilizes an attention layer [59], treating learnable prompts as a query and timestep embeddings as key and value, resulting in weighted prompts that are directly added to the latent vectors. Upon comparing the two gating architectures, we found that simple linear gating achieves better FID (5.87) compared to more sophisticated attention gating (6.41), which is actually worse than the baseline (6.27). As a result, we adopt linear gating as our default setting.

Gating type. In Table 3b, we evaluate two design choices for creating mixture-of-prompts: hard selection *vs.* soft selection. With hard selection, we choose the top- k prompts based on the gating function output probabilities, using them directly with a weight of 1. This explicitly separates the combination of prompts for each timestep. We set $k=192$ out of 256 prompts (75% of total prompts). On the other hand, soft selection uses all prompts but assigns different weights to each. Soft selection leads to further improvement, whereas hard selection results in performance that is actually worse than the base pre-trained model. Therefore, we set the soft selection as our default setting.

Prompt selection. By default, DMP inserts learnable prompts into the input space of every block of the diffusion model. Two choices arise in this context: (1) uniform: gating function \mathcal{G} in Eq. (5) receives only the timestep embedding t as input and applies output weights to the prompts at every block, thus prompt selection is consistent across all blocks. (2) distinct: \mathcal{G} processes not only t but also current block depth i as inputs, generating different weights for each block. As shown in Table 3c, using distinct prompt selections leads to enhanced performance. Therefore, we incorporate both the timestep embedding and current block depth information into the gating function, enabling the use of distinct prompt combinations for each block depth as our default setting.

Prompt position. Previous prompt tuning approaches [22, 29, 31, 61, 71] typically prepend learnable prompts to image tokens. In our work, we directly add prompts element-wise to image tokens, thereby maintaining the input sequence length. Table 3d ablates different choices for inserting prompts into the input space and their impact on performance. We compare two methods: prepend *vs.* add. For “add”, we use 256 prompts to match the number of image tokens, and for “prepend”, we utilize 50 prompts. Although ideally, “prepend” should also use 256 tokens for a fair comparison, we empirically found that prepending 256 prompt tokens causes diffusion models to diverge, even when both methods are initialized with zero equally. Hence, we limit “prepend” to 50 tokens. The

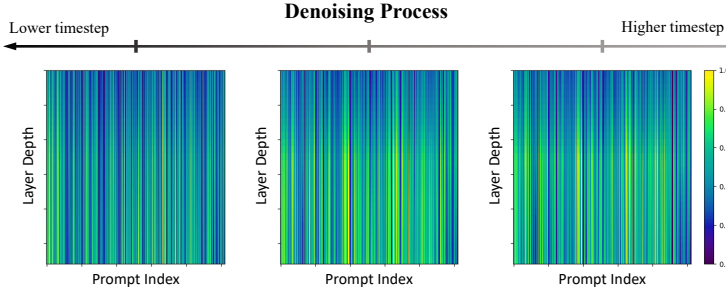


Figure 5: **Prompt activation.** Brighter means stronger activation.

Class-conditional (ImageNet)	
Model	FID↓
DiT-XL/2 (iter: 7M)	2.29
+ DMP (only t)	2.25
+ DMP ($t + c$)	2.25
Text-to-Image (MS-COCO)	
Model	FID↓
DiT-B/2 (iter: 450K)	7.33
+ DMP (only t)	7.30
+ DMP ($t + c$)	7.12

Table 5: **Gating condition.**

results show that while “add” method improves performance with a stable optimization process, achieving a 5.87 FID compared to the baseline of 6.27 FID. On the other hand, the “prepend” leads to a drop in performance, with an FID of 6.79. Additionally, “add” has the advantage of not increasing computation overhead. Based on these findings, we set “add” as our default for stable optimization.

Prompt balancing. Prompt balancing loss acts as a soft constraint for the gating function, helping to mitigate biased selections of prompts when producing a mixture-of-prompts. We study the effects of two types of balancing losses: importance balancing loss and load balancing loss. As shown in Table 3e, using both types of losses enables the diffusion model to reach its peak performance. When used individually, each type of loss contributes slightly to performance improvement, but when used together, they exhibit complementary effects, boosting overall performance. This indicates that balancing both the weight of the activated prompts and the number of activated prompts across different timesteps is crucial for creating an effective mixture-of-prompts. Consequently, we use both importance balancing loss and load balancing loss for prompt balancing.

4.3 Analysis

Prompt activation. The gating function plays a pivotal role in dynamically crafting mixtures-of-prompts from a set of learnable prompts, based on the noise level present in the input. This is depicted in Fig. 5, where the activation is visually highlighted using colors. As the denoising process progresses, the selection of prompts exhibits significant variation across different timesteps. At higher timesteps, where noise levels are greater, the gating function tends to utilize a broader array of prompts. Conversely, at lower timesteps, as the noise diminishes, the prompts become more specialized, focusing narrowly on specific features of the input that demand closer attention. This strategic deployment of prompts allows the model to form specialized “experts” at each denoising step. Such adaptability enables the model to adjust its approach based on the current noise level, effectively leveraging different prompts to enhance its overall performance. Using mixture-of-prompts tailored to different noise levels ensures that the image generation process is both flexible and precise, catering to the specific needs dictated by the input’s noise characteristics at each step.

Gating condition. In class-conditional image generation and text-to-image generation tasks, conditional guidance plays a crucial role in determining the outcome of generated images [8, 18]. To study the impact of conditional guidance on selecting mixtures-of-prompts, we evaluate the performances of two cases: one where the gating function \mathcal{G} receives only the timestep embedding t , and the other where it receives both t and the class or text condition embedding c . In the latter case, we modify the input of the gating function in Eq. (5), from t to $t + c$. Our analysis, presented in Section 4.2, indicates that on the ImageNet dataset, both methods perform equivalently, whereas on the COCO dataset, using $t + c$ yields superior performance compared to using t alone. This suggests that incorporating conditional guidance can help in determining how to combine prompts at each denoising step to generate an image that aligns well with the text condition. Consequently, we use $t + c$ as the default input for the gating function in the text-to-image task.

Qualitative analysis. Fig. 6 presents a visual comparison between three methods: the baseline DiT model, prompt tuning [29], and our DMP. These methods are evaluated on unconditional, text-to-image generation tasks using FFHQ [25] and COCO [33], respectively. Overall, DMP demon-

(a) Unconditional Image Generation on FFHQ [25]



(b) Text-to-Image Generation on MS-COCO [33].

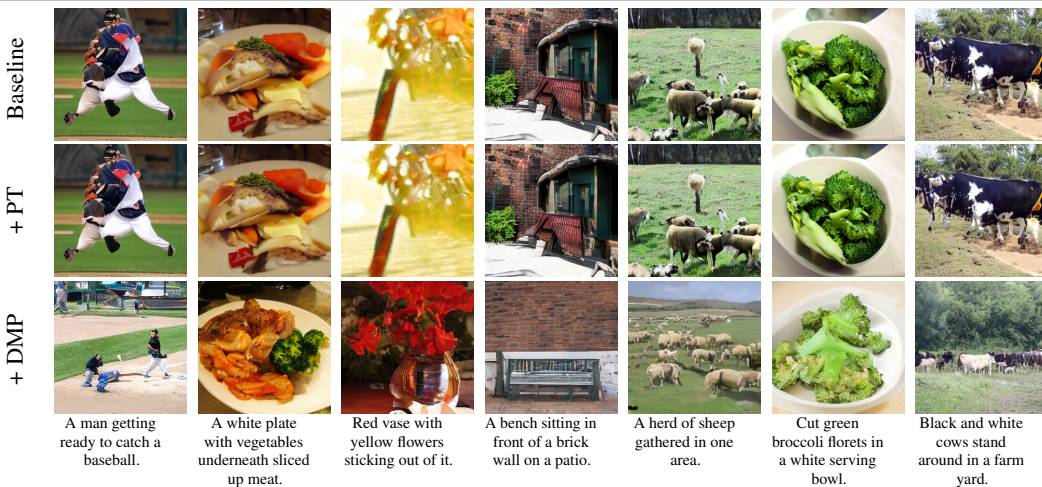


Figure 6: **Qualitative comparison** among the baseline (DiT-B/2 [43]), naive prompt tuning (PT) applied to the baseline [29], and DMP applied to the baseline on (a) FFHQ [25] and (b) MS-COCO [33] datasets.

strates realistic and natural images with fewer artifacts. We provide additional qualitative results in Appendix E.

5 Conclusion

In this study, we introduced Diffusion Model Patching (DMP), a lightweight and computationally efficient method for enhancing pre-trained diffusion models that have already converged. Most pre-trained diffusion models do not explicitly integrate denoising-stage-specificity into their model design. Given that the characteristics of denoising stages differ slightly, we aim to modify the model to be aware of such differences. The key idea is to integrate timestep-specific learnable prompts to patch the model’s behavior at every timestep. To achieve this, DMP leverages dynamic gating, which adaptively combines prompts based on the current timestep (or noise level) during the denoising process. This allows our method to scale effectively to thousands of denoising steps. Our results demonstrate that while fine-tuning the model on the original dataset does not lead to further improvement, DMP uniquely enhances performance. When applied to the DiT-XL backbone, DMP yields substantial FID gain of 10.38% in 50K iterations, with just 1.43% extra parameters on FFHQ 256×256 . Notably, DMP’s effectiveness extends across different model sizes and various image generation tasks.

Limitations. Our DMP method adopts a prompt-adding strategy to ensure stable training and maintain sampling speed. However, since the number of input patches is fixed, the flexibility in the number of prompts is limited. Extending our DMP with a prepend approach while maintaining stable training is an interesting future direction.

References

- [1] Hyojin Bahng, Ali Jahanian, Swami Sankaranarayanan, and Phillip Isola. Exploring visual prompts for adapting large-scale models. *arXiv preprint arXiv:2203.17274*, 2022.
- [2] Yogesh Balaji, Seungjun Nah, Xun Huang, Arash Vahdat, Jiaming Song, Karsten Kreis, Miika Aittala, Timo Aila, Samuli Laine, Bryan Catanzaro, et al. ediffi: Text-to-image diffusion models with an ensemble of expert denoisers. *arXiv preprint arXiv:2211.01324*, 2022.
- [3] Tom Brown, Benjamin Mann, Nick Ryder, Melanie Subbiah, Jared D Kaplan, Prafulla Dhariwal, Arvind Neelakantan, Pranav Shyam, Girish Sastry, Amanda Askell, et al. Language models are few-shot learners. *Advances in neural information processing systems*, 33:1877–1901, 2020.
- [4] Rich Caruana. Multitask learning. *Machine learning*, 28:41–75, 1997.
- [5] Shoufa Chen, Chongjian Ge, Zhan Tong, Jiangliu Wang, Yibing Song, Jue Wang, and Ping Luo. Adapt-former: Adapting vision transformers for scalable visual recognition. *Advances in Neural Information Processing Systems*, 35:16664–16678, 2022.
- [6] Jooyoung Choi, Jungbeom Lee, Chaehun Shin, Sungwon Kim, Hyunwoo Kim, and Sungroh Yoon. Perception prioritized training of diffusion models. In *Proceedings of the IEEE/CVF Conference on Computer Vision and Pattern Recognition*, pages 11472–11481, 2022.
- [7] Jia Deng, Wei Dong, Richard Socher, Li-Jia Li, Kai Li, and Li Fei-Fei. Imagenet: A large-scale hierarchical image database. In *2009 IEEE conference on computer vision and pattern recognition*, pages 248–255. Ieee, 2009.
- [8] Prafulla Dhariwal and Alexander Nichol. Diffusion models beat gans on image synthesis. *Advances in neural information processing systems*, 34:8780–8794, 2021.
- [9] David Eigen, Marc’Aurelio Ranzato, and Ilya Sutskever. Learning factored representations in a deep mixture of experts. *arXiv preprint arXiv:1312.4314*, 2013.
- [10] Zhida Feng, Zhenyu Zhang, Xintong Yu, Yewei Fang, Lanxin Li, Xuyi Chen, Yuxiang Lu, Jiaxiang Liu, Weichong Yin, Shikun Feng, et al. Ernie-vilg 2.0: Improving text-to-image diffusion model with knowledge-enhanced mixture-of-denoising-experts. In *Proceedings of the IEEE/CVF Conference on Computer Vision and Pattern Recognition*, pages 10135–10145, 2023.
- [11] Rinon Gal, Yuval Alaluf, Yuval Atzmon, Or Patashnik, Amit H Bermano, Gal Chechik, and Daniel Cohen-Or. An image is worth one word: Personalizing text-to-image generation using textual inversion. *arXiv preprint arXiv:2208.01618*, 2022.
- [12] Hyojun Go, JinYoung Kim, Yunsung Lee, Seunghyun Lee, Shinhyeok Oh, Hyeongdon Moon, and Seungtaek Choi. Addressing negative transfer in diffusion models. *arXiv preprint arXiv:2306.00354*, 2023.
- [13] Ligong Han, Yinxiao Li, Han Zhang, Peyman Milanfar, Dimitris Metaxas, and Feng Yang. Svdiff: Compact parameter space for diffusion fine-tuning. *arXiv preprint arXiv:2303.11305*, 2023.
- [14] Tiankai Hang, Shuyang Gu, Chen Li, Jianmin Bao, Dong Chen, Han Hu, Xin Geng, and Baining Guo. Efficient diffusion training via min-snr weighting strategy. *arXiv preprint arXiv:2303.09556*, 2023.
- [15] Amir Hertz, Ron Mokady, Jay Tenenbaum, Kfir Aberman, Yael Pritch, and Daniel Cohen-Or. Prompt-to-prompt image editing with cross attention control. *arXiv preprint arXiv:2208.01626*, 2022.
- [16] Martin Heusel, Hubert Ramsauer, Thomas Unterthiner, Bernhard Nessler, and Sepp Hochreiter. Gans trained by a two time-scale update rule converge to a local nash equilibrium. *Advances in neural information processing systems*, 30, 2017.
- [17] Jonathan Ho, Ajay Jain, and Pieter Abbeel. Denoising diffusion probabilistic models. *Advances in neural information processing systems*, 33:6840–6851, 2020.
- [18] Jonathan Ho and Tim Salimans. Classifier-free diffusion guidance. *arXiv preprint arXiv:2207.12598*, 2022.
- [19] Neil Houlsby, Andrei Giurgiu, Stanislaw Jastrzebski, Bruna Morrone, Quentin De Laroussilhe, Andrea Gesmundo, Mona Attariyan, and Sylvain Gelly. Parameter-efficient transfer learning for nlp. In *International Conference on Machine Learning*, pages 2790–2799. PMLR, 2019.

- [20] Edward J Hu, Yelong Shen, Phillip Wallis, Zeyuan Allen-Zhu, Yuanzhi Li, Shean Wang, Lu Wang, and Weizhu Chen. Lora: Low-rank adaptation of large language models. *arXiv preprint arXiv:2106.09685*, 2021.
- [21] Robert A Jacobs, Michael I Jordan, Steven J Nowlan, and Geoffrey E Hinton. Adaptive mixtures of local experts. *Neural computation*, 3(1):79–87, 1991.
- [22] Menglin Jia, Luming Tang, Bor-Chun Chen, Claire Cardie, Serge Belongie, Bharath Hariharan, and Ser-Nam Lim. Visual prompt tuning. In *European Conference on Computer Vision*, pages 709–727. Springer, 2022.
- [23] Zeyinzi Jiang, Chaojie Mao, Yulin Pan, Zhen Han, and Jingfeng Zhang. Scedit: Efficient and controllable image diffusion generation via skip connection editing. *arXiv preprint arXiv:2312.11392*, 2023.
- [24] Michael I Jordan and Robert A Jacobs. Hierarchical mixtures of experts and the em algorithm. *Neural computation*, 6(2):181–214, 1994.
- [25] Tero Karras, Samuli Laine, and Timo Aila. A style-based generator architecture for generative adversarial networks. In *Proceedings of the IEEE/CVF conference on computer vision and pattern recognition*, pages 4401–4410, 2019.
- [26] Diederik P Kingma and Max Welling. Auto-encoding variational bayes. *arXiv preprint arXiv:1312.6114*, 2013.
- [27] Zhifeng Kong, Wei Ping, Jiaji Huang, Kexin Zhao, and Bryan Catanzaro. Diffwave: A versatile diffusion model for audio synthesis. *arXiv preprint arXiv:2009.09761*, 2020.
- [28] Nupur Kumari, Bingliang Zhang, Richard Zhang, Eli Shechtman, and Jun-Yan Zhu. Multi-concept customization of text-to-image diffusion. In *Proceedings of the IEEE/CVF Conference on Computer Vision and Pattern Recognition*, pages 1931–1941, 2023.
- [29] Brian Lester, Rami Al-Rfou, and Noah Constant. The power of scale for parameter-efficient prompt tuning. *arXiv preprint arXiv:2104.08691*, 2021.
- [30] Xiang Li, John Thickstun, Ishaan Gulrajani, Percy S Liang, and Tatsunori B Hashimoto. Diffusion-lm improves controllable text generation. *Advances in Neural Information Processing Systems*, 35:4328–4343, 2022.
- [31] Xiang Lisa Li and Percy Liang. Prefix-tuning: Optimizing continuous prompts for generation. *arXiv preprint arXiv:2101.00190*, 2021.
- [32] Dongze Lian, Daquan Zhou, Jiashi Feng, and Xinchao Wang. Scaling & shifting your features: A new baseline for efficient model tuning. *Advances in Neural Information Processing Systems*, 35:109–123, 2022.
- [33] Tsung-Yi Lin, Michael Maire, Serge Belongie, James Hays, Pietro Perona, Deva Ramanan, Piotr Dollár, and C Lawrence Zitnick. Microsoft coco: Common objects in context. In *Computer Vision—ECCV 2014: 13th European Conference, Zurich, Switzerland, September 6–12, 2014, Proceedings, Part V 13*, pages 740–755. Springer, 2014.
- [34] Pengfei Liu, Weizhe Yuan, Jinlan Fu, Zhengbao Jiang, Hiroaki Hayashi, and Graham Neubig. Pre-train, prompt, and predict: A systematic survey of prompting methods in natural language processing. *ACM Computing Surveys*, 55(9):1–35, 2023.
- [35] Xiao Liu, Kaixuan Ji, Yicheng Fu, Weng Lam Tam, Zhengxiao Du, Zhilin Yang, and Jie Tang. P-tuning v2: Prompt tuning can be comparable to fine-tuning universally across scales and tasks. *arXiv preprint arXiv:2110.07602*, 2021.
- [36] Xiao Liu, Yanan Zheng, Zhengxiao Du, Ming Ding, Yujie Qian, Zhilin Yang, and Jie Tang. Gpt understands, too. *AI Open*, 2023.
- [37] Robert L Logan IV, Ivana Balažević, Eric Wallace, Fabio Petroni, Sameer Singh, and Sebastian Riedel. Cutting down on prompts and parameters: Simple few-shot learning with language models. *arXiv preprint arXiv:2106.13353*, 2021.
- [38] Ilya Loshchilov and Frank Hutter. Decoupled weight decay regularization. *arXiv preprint arXiv:1711.05101*, 2017.

- [39] Chong Mou, Xintao Wang, Liangbin Xie, Jian Zhang, Zhongang Qi, Ying Shan, and Xiaohu Qie. T2i-adapter: Learning adapters to dig out more controllable ability for text-to-image diffusion models. *arXiv preprint arXiv:2302.08453*, 2023.
- [40] Alexander Quinn Nichol and Prafulla Dhariwal. Improved denoising diffusion probabilistic models. In *International Conference on Machine Learning*, pages 8162–8171. PMLR, 2021.
- [41] Sinno Jialin Pan and Qiang Yang. A survey on transfer learning. *IEEE Transactions on knowledge and data engineering*, 22(10):1345–1359, 2009.
- [42] Byeongjun Park, Sangmin Woo, Hyojun Go, Jin-Young Kim, and Changick Kim. Denoising task routing for diffusion models. *arXiv preprint arXiv:2310.07138*, 2023.
- [43] William Peebles and Saining Xie. Scalable diffusion models with transformers. *arXiv preprint arXiv:2212.09748*, 2022.
- [44] Fabio Petroni, Tim Rocktäschel, Patrick Lewis, Anton Bakhtin, Yuxiang Wu, Alexander H Miller, and Sebastian Riedel. Language models as knowledge bases? *arXiv preprint arXiv:1909.01066*, 2019.
- [45] Ben Poole, Ajay Jain, Jonathan T Barron, and Ben Mildenhall. Dreamfusion: Text-to-3d using 2d diffusion. *arXiv preprint arXiv:2209.14988*, 2022.
- [46] Alec Radford, Jeffrey Wu, Rewon Child, David Luan, Dario Amodei, Ilya Sutskever, et al. Language models are unsupervised multitask learners. *OpenAI blog*, 1(8):9, 2019.
- [47] Aditya Ramesh, Mikhail Pavlov, Gabriel Goh, Scott Gray, Chelsea Voss, Alec Radford, Mark Chen, and Ilya Sutskever. Zero-shot text-to-image generation. In *International Conference on Machine Learning*, pages 8821–8831. PMLR, 2021.
- [48] Robin Rombach, Andreas Blattmann, Dominik Lorenz, Patrick Esser, and Björn Ommer. High-resolution image synthesis with latent diffusion models. In *Proceedings of the IEEE/CVF Conference on Computer Vision and Pattern Recognition*, pages 10684–10695, 2022.
- [49] Nataniel Ruiz, Yuanzhen Li, Varun Jampani, Yael Pritch, Michael Rubinstein, and Kfir Aberman. Dream-booth: Fine tuning text-to-image diffusion models for subject-driven generation. In *Proceedings of the IEEE/CVF Conference on Computer Vision and Pattern Recognition*, pages 22500–22510, 2023.
- [50] Chitwan Saharia, William Chan, Saurabh Saxena, Lala Li, Jay Whang, Emily L Denton, Kamyar Ghasemipour, Raphael Gontijo Lopes, Burcu Karagol Ayan, Tim Salimans, et al. Photorealistic text-to-image diffusion models with deep language understanding. *Advances in Neural Information Processing Systems*, 35:36479–36494, 2022.
- [51] Chitwan Saharia, Jonathan Ho, William Chan, Tim Salimans, David J Fleet, and Mohammad Norouzi. Image super-resolution via iterative refinement. *IEEE Transactions on Pattern Analysis and Machine Intelligence*, 45(4):4713–4726, 2022.
- [52] Timo Schick and Hinrich Schütze. It’s not just size that matters: Small language models are also few-shot learners. *arXiv preprint arXiv:2009.07118*, 2020.
- [53] Noam Shazeer, Azalia Mirhoseini, Krzysztof Maziarz, Andy Davis, Quoc Le, Geoffrey Hinton, and Jeff Dean. Outrageously large neural networks: The sparsely-gated mixture-of-experts layer. *arXiv preprint arXiv:1701.06538*, 2017.
- [54] Jascha Sohl-Dickstein, Eric Weiss, Niru Maheswaranathan, and Surya Ganguli. Deep unsupervised learning using nonequilibrium thermodynamics. In *International conference on machine learning*, pages 2256–2265. PMLR, 2015.
- [55] Jiaming Song, Chenlin Meng, and Stefano Ermon. Denoising diffusion implicit models. *arXiv preprint arXiv:2010.02502*, 2020.
- [56] Yang Song and Stefano Ermon. Generative modeling by estimating gradients of the data distribution. *Advances in neural information processing systems*, 32, 2019.
- [57] Yi-Lin Sung, Jaemin Cho, and Mohit Bansal. Lst: Ladder side-tuning for parameter and memory efficient transfer learning. *Advances in Neural Information Processing Systems*, 35:12991–13005, 2022.
- [58] Christian Szegedy, Vincent Vanhoucke, Sergey Ioffe, Jon Shlens, and Zbigniew Wojna. Rethinking the inception architecture for computer vision. In *Proceedings of the IEEE conference on computer vision and pattern recognition*, pages 2818–2826, 2016.

- [59] Ashish Vaswani, Noam Shazeer, Niki Parmar, Jakob Uszkoreit, Llion Jones, Aidan N Gomez, Łukasz Kaiser, and Illia Polosukhin. Attention is all you need. *Advances in neural information processing systems*, 30, 2017.
- [60] Pascal Vincent. A connection between score matching and denoising autoencoders. *Neural computation*, 23(7):1661–1674, 2011.
- [61] Zifeng Wang, Zizhao Zhang, Chen-Yu Lee, Han Zhang, Ruoxi Sun, Xiaoqi Ren, Guolong Su, Vincent Perot, Jennifer Dy, and Tomas Pfister. Learning to prompt for continual learning. In *Proceedings of the IEEE/CVF Conference on Computer Vision and Pattern Recognition*, pages 139–149, 2022.
- [62] Sangmin Woo, Byeongjun Park, Hyojun Go, Jin-Young Kim, and Changick Kim. Harmonyview: Harmonizing consistency and diversity in one-image-to-3d. *arXiv preprint arXiv:2312.15980*, 2023.
- [63] Chendong Xiang, Fan Bao, Chongxuan Li, Hang Su, and Jun Zhu. A closer look at parameter-efficient tuning in diffusion models. *arXiv preprint arXiv:2303.18181*, 2023.
- [64] Enze Xie, Lewei Yao, Han Shi, Zhili Liu, Daquan Zhou, Zhaoqiang Liu, Jiawei Li, and Zhenguo Li. Difffit: Unlocking transferability of large diffusion models via simple parameter-efficient fine-tuning. *arXiv preprint arXiv:2304.06648*, 2023.
- [65] Runxin Xu, Fuli Luo, Zhiyuan Zhang, Chuanqi Tan, Baobao Chang, Songfang Huang, and Fei Huang. Raise a child in large language model: Towards effective and generalizable fine-tuning. *arXiv preprint arXiv:2109.05687*, 2021.
- [66] Zeyue Xue, Guanglu Song, Qiushan Guo, Boxiao Liu, Zhuofan Zong, Yu Liu, and Ping Luo. Raphael: Text-to-image generation via large mixture of diffusion paths. *arXiv preprint arXiv:2305.18295*, 2023.
- [67] Elad Ben Zaken, Shauli Ravfogel, and Yoav Goldberg. Bitfit: Simple parameter-efficient fine-tuning for transformer-based masked language-models. *arXiv preprint arXiv:2106.10199*, 2021.
- [68] Jeffrey O Zhang, Alexander Sax, Amir Zamir, Leonidas Guibas, and Jitendra Malik. Side-tuning: a baseline for network adaptation via additive side networks. In *Computer Vision—ECCV 2020: 16th European Conference, Glasgow, UK, August 23–28, 2020, Proceedings, Part III 16*, pages 698–714. Springer, 2020.
- [69] Lvmin Zhang, Anyi Rao, and Maneesh Agrawala. Adding conditional control to text-to-image diffusion models. In *Proceedings of the IEEE/CVF International Conference on Computer Vision*, pages 3836–3847, 2023.
- [70] Kaiyang Zhou, Jingkang Yang, Chen Change Loy, and Ziwei Liu. Conditional prompt learning for vision-language models. In *Proceedings of the IEEE/CVF Conference on Computer Vision and Pattern Recognition*, pages 16816–16825, 2022.
- [71] Kaiyang Zhou, Jingkang Yang, Chen Change Loy, and Ziwei Liu. Learning to prompt for vision-language models. *International Journal of Computer Vision*, 130(9):2337–2348, 2022.

Appendix

A Additional Related Work

Prompt-based learning. Recent progress in NLP has shifted towards leveraging pre-trained language models (LMs) using textual prompts [34, 44, 46, 52] to guide models to perform target tasks or produce desired outputs without additional task-specific training. With strategically designed prompts, models like GPT-3 [3] have shown impressive generalization across various downstream tasks, even under few-shot or zero-shot conditions. Prompt tuning [29, 31, 35, 36] treats prompts as learnable parameters optimized with supervision signals from downstream training samples while keeping the LM’s parameters fixed. Similar principles have also been explored in visual [1, 22] and vision-and-language [70, 71] domains. To the best of our knowledge, there is currently no direct extension of prompt tuning in enhancing the in-domain performance of diffusion models. While Prompt2prompt [15] and Textual Inversion [11] share similar properties with prompt tuning, their focus is on customized editing or personalized content generation. In this work, we propose to leverage prompt tuning to enhance the stage-specific capabilities of diffusion models. With only a small number of prompts, we can effectively scale to thousands of denoising steps via a mixture-of-prompts strategy.

B Preliminary

Diffusion models. Diffusion models [8, 55] generate data by reversing a pre-defined diffusion process (or *forward process*), which sequentially corrupts the original data \mathbf{x}_0 into noise over a series of steps $t \in \{1, \dots, T\}$.

$$q(\mathbf{x}_t|\mathbf{x}_{t-1}) = \mathcal{N}(\mathbf{x}_t; \sqrt{1 - \beta_t}\mathbf{x}_{t-1}, \beta_t\mathbf{I}), \quad (7)$$

where $0 < \beta_t < 1$ is a variance schedule controlling the amount of noise added at each step. This process results in data that resembles pure noise $\mathcal{N}(0, \mathbf{I})$ at step T (often $T = 1000$). The *reverse process* aims to reconstruct the original data by denoising, starting from noise and moving backward to the initial state \mathbf{x}_0 . This is modeled by a neural network parameterized by θ that learns the conditional distribution $p_\theta(\mathbf{x}_{t-1}|\mathbf{x}_t)$. The network is trained by optimizing a weighted sum [17] of denoising score matching losses [60] over multiple noise scales [56]. In practice, the network predicts the noise ϵ added at each forward step, rather than directly predicting \mathbf{x}_{t-1} from \mathbf{x}_t , using the objective function:

$$\mathcal{L}_t := \mathbb{E}_{\mathbf{x}_0, \epsilon \sim \mathcal{N}(0,1), t \sim U[1,T]} \|\epsilon - \epsilon_\theta(\mathbf{x}_t, t)\|_2^2. \quad (8)$$

By minimizing Eq. (8) for all t , the neural network learns to effectively reverse the noising process, thereby enabling itself to generate samples from $p_\theta(\mathbf{x}_0)$ that closely resemble the original data distribution.

C Prompt Balancing Loss

During the training stage of our DMP method, we adopt a prompt balancing loss to prevent the gate from selecting only a few specific prompts, a problem known as mode collapse. The prompt balancing loss is inspired by the balancing loss used in mixture-of-experts. Our prompt balancing loss includes the importance loss, which ensures prompts are selected uniformly within a batch, and the load balancing loss, which prevents the existence of unselected prompts in a batch. When defining the n -th prompt gating in the i -th DiT-block layer as g_n^i , the formulations of the importance loss and load balancing loss are as follows:

$$\mu_i = \frac{1}{N} \sum_{n=0}^{N-1} g_n^i, \quad \sigma_i = \frac{1}{N} \sum_{n=0}^{N-1} (g_n^i - \mu_i)^2 \quad (9)$$

$$L_{importance} = \sum_{i=0}^{L-1} \frac{\sigma_i}{\mu_i^2 + \epsilon}, \quad L_{Load} = \frac{1}{L} \sum_{i=0}^{L-1} I(g_n^i < 0), \quad (10)$$

where L is the total number of DiT block layers, N is the total number of prompts, ϵ is $1e^{-5}$ to prevent division by zero, and I is the indicator function that counts the number of elements satisfying the condition ($g_n^i > 0$). The importance loss uses the squared coefficient of variation, which makes the variance value robust against the mean value. With these prompt balancing losses, we regularize the prompt selection in the gate, ensuring that there are few unselected prompts, as shown in Fig. 5 of main manuscript.

D Implementation Details

Our experiments followed this setup for further training of pretrained DiT-B/L/XL models [43]. Firstly, we used a diffusion timestep T of 1000 for training and DDPM with 250 steps [17] for sampling. For beta scheduling, cosine scheduling [40] was used for the FFHQ [25] and MS-COCO datasets [33], while linear scheduling was used for the ImageNet dataset [7]. For text-to-image generation (MS-COCO) and class-conditional image generation (ImageNet) tasks, we adopted classifier-free guidance [18] with a guidance scale of 1.5. The batch size was set to 128, and random horizontal flipping was applied to the training data. We used the AdamW optimizer [38] with a fixed learning rate of $1e-4$ and no weight decay. Originally, the exponential moving average (EMA) technique is utilized for stable training of DiT models. However, since our method involves further training on pretrained models with only a few training steps, we did not adopt the EMA strategy. All experiments were conducted using a single NVIDIA A100 GPU.

E Additional Qualitative Results on ImageNet

Figures 7 to 10 illustrates the generated images by pre-trained DiT-XL with DMP trained on 50K iterations. The results demonstrate that highly realistic images can be generated, even with relatively limited training.



Figure 7: **Uncurated 256x256 DiT-XL/2+DMP samples.**
Classifier-free guidance scale = 1.5.
Class label = "golden retriever" (207)



Figure 8: **Uncurated 256x256 DiT-XL/2+DMP samples.**
Classifier-free guidance scale = 1.5.
Class label = "goldfish" (1)



Figure 9: **Uncurated 256x256 DiT-XL/2+DMP samples.**
Classifier-free guidance scale = 1.5.
Class label = "hummingbird" (94)



Figure 10: Uncurated 256×256 DiT-XL/2+DMP samples.
Classifier-free guidance scale = 1.5.
Class label = “ostrich” (9)